THEORETICAL AND EXPERIMENTAL STUDIES OF CAMBERED AND TWISTED

WINGS OPTIMIZED FOR FLIGHT AT SUPERSONIC SPEEDS

By Clinton E. Brown, F. E. McLean, and E. B. Klunker

For Presentation at the Second International Congress of the
Institute of the Aeronautical Sciences

Zurich, Switzerland
September 12-16, 1960

(3)

THEORETICAL AND EXPERIMENTAL STUDIES OF CAMBERED AND TWISTED

WINGS OPTIMIZED FOR FLIGHT AT SUPERSONIC SPEEDS

By Clinton E. Brown*, F. E. McLean**, and E. B. Klunker**

, NASA Langley Research Center

ABSTRACT

It is known that linearized theory predicts very low values of drag
due to lift at supersonic speeds when proper planform and load distribu-
tion are used. Attempts to obtain these predicted values experimentally
have met with very limited success. The failure of the linearized theory
is shown to result from the attainment of a supercritical flow over the
wings, an effect which is beyond the scope of simple first-order theory.
By consideration of second-order terms in the pressure equation, analysis
indicates that it is extremely difficult to design a cambered and twisted
sweptback wing that would avoid supercritical flow at realistic lift
coefficients. Nevertheless, a series of sweptback wings have been
designed and tested in order to verify the analysis, and results of this
investigation are described. Other approaches to the problem involve the
use of supersonic edged wings preceded by fuselage-like lifting bodies.
An analysis of such configurations is presented including the develop-
ment of a new method for calculating optimized loadings on wings of
arbitrary planform. It is shown to be necessary to account for combined
lifting and volume effects in the design of such configurations.

---

*Chief, Theoretical Mechanics Division.

**Aeronautical Research Engineer.

L-1245

INTRODUCTION

The present report is concerned with researches carried out over the past few years to understand the complex flows about wings at supersonic transport speeds and to utilize this understanding in an attempt to design wings and wing-body configurations of high aerodynamic efficiency. Basic research over the past decade has been conducted in flight, in high-speed wind tunnels, and by analysis, and the agglomeration of these results has given us today the ability to design supersonic transports for $M \approx 3$ having lift-to-drag ratios in the range from 7 to 8. In the design of sweptback wings, however, there is one frustrating area of research in which the theoretical predictions of favorable drag-due-to-lift reductions have not been experimentally confirmed (ref. 1). There arises then the important question of whether the gains predicted by linearized theory are attainable in nature or are only manifestations of our mathematical imagination. Study of the problem through analysis is required since the unlimited possibilities for cambered surface shapes makes the pure experimental approach too costly. Some progress has been made on the nonlinear problem, references 2 through 5; however, the basic equations of interest are of the mixed elliptic and hyperbolic type (see Ferri, Voglio-Laurin, and Ness, ref. 2) and are even more intractable than the unsolved problem of two-dimensional transonic flow. In this paper some experimental results are given for wings designed according to linear theory together with an analysis of the expected effects of the nonlinear aerodynamics.

DISCUSSION OF THE PROBLEM

A great deal of research effort has been expended in attempts to realize the favorable drag-due-to-lift characteristics predicted by linear theory for flat arrow wings with subsonic leading edges. The favorable characteristics of this type of wing are predicated on the basis of a leading-edge thrust force which is attributed to the infinite leading-edge suction associated with the flat-plate loading. As pointed out in reference 1, this predicted leading-edge thrust has rarely been found to any reasonable extent in experimental tests of flat wings. However, in recent years many investigators (refs. 6, 7, 8, and 9) have espoused the idea that an "optimum" loaded surface can be obtained, within the framework of linear theory, which will effectively attain or exceed the favorable drag-due-to-lift characteristics of the flat wing without dependency on leading-edge thrust and with finite pressures everywhere on the surface. Several experimental tests of these optimum cambered wings have indicated fairly high levels of lift-to-drag ratio (refs. 10 and 11); however, the good overall efficiency can be attributed to the low minimum drags associated with highly swept arrow wings and, in some cases, laminar flow rather than the attainment of the predicted qualities of low drag due to lift.

In reference 1 several possible reasons were given for the failure of the optimum cambered wings to produce the low values of drag due to lift predicted by theory. First, the basic nature of the loading over the optimum surface is such that the leading-edge pressures on the upper surface, though finite, reach relatively high negative values. The

apparent effect of these high negative pressures is to induce a transonic or supercritical flow regime perpendicular to the wing leading edge and thus alter the pressure distribution from that expected. Second, since the optimum camber surface requires a careful balance between wing slope and pressure, the deviation due to transonic effects will certainly cause a rapid drag rise similar to that found experimentally on two-dimensional cambered airfoil sections as the critical speed was exceeded.

The transonic nature of the cross flow over the upper surface of an optimum wing was visible in an oil-film picture first presented in reference 1 and shown herein as figure 1. This photograph, taken in the Langley Unitary Plan wind tunnel, shows the half-wing in the tunnel with flow from left to right. It would appear that the shock-induced separation at the first white line was largely responsible for the failure of the wing to produce the low drag-due-to-lift performance predicted by theory. The wing, in fact, was not as efficient as an uncambered wing of the same planform and thickness distribution.

Because of the unpredicted drag rise that can reasonably be attributed to a transonic or supercritical cross flow on the upper surface of highly swept optimum wings, a theoretical and experimental research program was instituted at the Langley Research Center of the National Aeronautics and Space Administration in order to gain a better understanding of this flow regime. The basic questions to be investigated were: In the design of highly swept wing surfaces, what restrictions are necessary to minimize the possible adverse transonic cross-flow effects? And, will the severity of the required restriction negate the possible attainment of some of the favorable drag-due-to-lift

characteristics predicted by theory? The first part of this paper will

discuss the results of this combined research program as they apply to

these questions.

CRITICAL SPEED FOR SUPERSONIC SWEPTBACK WINGS

Since, from all appearances, the most critical region in the design

of highly swept optimum cambered wings is on the upper surface near the

leading edge, in the analysis primary attention has been given to this

specific region. For this region, an approximation of the restrictions

necessary to delay the onset of induced critical cross flow can be

obtained through the use of simple swept theory.

From simple sweep considerations the pressure coefficient which will

induce sonic flow normal to the leading edge of a wing swept Λ degrees

and flying at a stream Mach number, M, is given by

$$C_{p,sonic} = -\frac{2}{\gamma M^2}\left\{1 - \left[\frac{2 + (\gamma - 1)M^2\cos^2\Lambda}{1 + \gamma}\right]^{\frac{\gamma}{\gamma-1}}\right\} \qquad (1)$$

where γ is the ratio of specific heats and is taken as 1.4. Since the

basic purpose of the optimum design approach is to obtain minimum drag

for a given lift, it is convenient in the analysis to relate the critical

pressure coefficient given by equation (1) to the lift coefficient. It

is also convenient to establish the critical lift coefficient for a

uniformly loaded surface, keeping in mind that the leading-edge pressures

for optimum wings are considerably greater than the average over the

surface.

Again, using simple sweep theory for a uniformly loaded surface we can obtain the approximate expressions

$$u = \frac{C_L}{4}$$

and

$$v = -\frac{C_L}{4} \tan \Lambda \tag{2}$$

where u and v are the ratios of the upper surface, streamwise and lateral perturbation velocities to the freestream velocity, and C_L is the lift coefficient.

Since to first-order $C_p = -2u = -\frac{C_L}{2}$, we can, with the use of equation (1), determine a first-order critical lift coefficient for uniform loading given by

$$C_{L,1}^* = \frac{4}{\gamma M^2} \left\{ 1 - \left[\frac{2 + (\gamma - 1)M^2 \cos^2\Lambda}{1 + \gamma} \right]^{\frac{\gamma}{\gamma-1}} \right\} \tag{3}$$

A rough approximation to the second-order effects can be secured from the relation $C_p = -(2u + v^2) = -\left[\frac{C_L}{2} + \frac{C_L^2}{16} \tan^2\Lambda \right]$ which with equation (1) yields a second-order critical lift coefficient for uniform loading given by

$$C_{L,2}^* = 4 \left[\cot \Lambda \sqrt{ \cot^2\Lambda + \frac{2}{\gamma M^2} \left\{ 1 - \left[\frac{2 + (\gamma - 1)M^2 \cos^2\Lambda}{1 + \gamma} \right]^{\frac{\gamma}{\gamma-1}} \right\} } - \cot^2\Lambda \right] \tag{4}$$

The variation of the critical lift coefficients $C_{L,1}^*$ and $C_{L,2}^*$ with leading-edge sweep angle is shown in figure 2 for several Mach

numbers of current interest. From the simple considerations outlined above, it can be seen that even for the case of uniform loading rather high sweep angles are necessary to avert the onset of critical cross flow if reasonable lift coefficients are to be maintained. It is important to note that while the maximum critical lift coefficient is larger for the lower Mach numbers, the optimum design lift coefficient of supersonic transport airplanes also follows this trend and hence the critical speed problem is nearly as severe at $M = 2$ as at $M = 3$. Since the loading near the leading edge of an optimum wing is higher than the average over the surface, rather severe restrictions in overall lift or in load distribution are necessary to avoid supercritical flow and attendant flow-field distortion.

MODIFICATION OF OPTIMUM LOADINGS

Just how these restrictions apply to the camber of a specific planform is presented in figure 3. Here the upper-surface pressures due to camber, plotted as $-\dfrac{2C_{p,\text{upper}}}{C_{L,1}^{*}}$, are shown for a highly swept planform. The design Mach number is 3.0, the leading-edge sweep is $80°$, and the design lift coefficient is 0.08. The local chord position $\left(\dfrac{x}{c}\right) = 0.1$ in combination with the semispan stations $\dfrac{y}{s}$ defines a region very near the leading edge of the planform. Upper-surface pressures which lie above the line labeled $C_{L,1}^{*}$ indicate that the induced cross flow would be supercritical from first-order considerations. Upper-surface pressures which lie above the line labeled $C_{L,2}^{*}$

indicate that the cross flow would be supercritical from second-order considerations.

It can be seen from the figure that the optimum cambered surface, which has a theoretical drag rise factor, $\dfrac{C_D}{\beta C_L{}^2}$ of 0.167 is in a supercritical cross-flow regime from either first- or second-order considerations. On the other hand, the same planform cambered for uniform loading is in a subcritical flow regime, but has a relatively high drag rise factor of 0.223. Similar analyses of other sweptback planforms and design conditions indicated the same general trends. The optimum surface with low theoretical drag rise factors was in a super-critical cross flow, whereas uniformly loaded wings, in general, produced relatively high drag rise factors. Because of the probable adverse effects of supercritical cross flow pointed out earlier, neither of these two extreme design conditions would offer much hope for the attainment of favorable drag-due-to-lift characteristics without sizable additional effects such as thickness or interference bodies placed on the cambered surface. Consequently, an analysis was made to determine whether a camber loading could be obtained which would offer substantial relief from the leading-edge critical-flow problem with only small loss in theoretical drag-due-to-lift capability as compared with the optimum. Using a pressure superposition method similar to those described in references 12 and 13, it was found that, for a number of planforms and design conditions, the upper-surface pressures near the leading edge could be restricted to the first-order critical with only about a 10-percent increase in drag rise factor over that of the corresponding

- 8 -

optimum surface. For example, the restricted camber loading which has the leading-edge pressure distribution shown on figure 3, has a theoretical drag rise factor of 0.184 compared to 0.167 for the optimum camber loading.

EXPERIMENTAL MODELS AND THICKNESS EFFECTS

In order to determine what favorable effects, if any, might result from this restriction of the upper-surface pressures near the leading edge, a series of models was constructed to investigate the restricted design approach. In the design of the models an attempt was made to further reduce the upper-surface pressures through thickness effects. It was anticipated that a profile with sharp leading edges would be most favorable from the standpoint of producing a desired positive pressure increment on the upper surface near the leading edge. With no further consideration a circular-arc airfoil section was selected. Surprisingly, a search of the literature revealed that no calculated pressure distributions were available for circular-arc profiles on fully tapered swept-back wings. Subsequently, the method of Kainer (ref. 14) was used to calculate the desired circular-arc thickness pressures. The results of these calculations as they might influence the critical-flow region near the leading edge are shown in figure 4. The upper-surface pressures plotted as $\dfrac{-2C_{p,upper}}{C_{L,1}^{*}}$ are shown for a region near the leading edge of the same highly swept planform considered in the previous figure. It can be seen that a 2.5-percent-thick circular-arc profile when applied to the restricted cambered surface would theoretically bring the pressures

- 9 -

in the forward region of the leading edge to values below the second-order critical. However, as the tip is approached the desired effect is lost and there is an increase in negative pressure level. From leading-edge flow considerations it appears that a double-wedge profile of like thickness ratio would have been a better choice of thickness profile, although there might be adverse effects on the aft portion of the wing due to the ridge lines. Unfortunately, from considerations of shop availability and construction time, the experimental models for investigation of the restricted camber design philosophy were fabricated prior to the availability of thickness calculations. Consequently, on the simple sweep basis used in the analysis, only one of the cambered models had a completely subcritical leading edge at the design condition. The other cambered models had essentially the same leading-edge pressure distribution as that shown on figure 4 for the restricted camber with circular-arc thickness distribution.

A summary of the planforms and design conditions considered in the experimental investigation is shown in figure 5. All the wings were fully tapered arrow wings with a notch ratio equal to 35 percent of the overall length as shown on the figure. For tests at $M = 2$, wings with 70° and 75° leading-edge sweep were constructed, and for tests at $M = 3.0$, 80° of leading-edge sweep was used. The cambered surfaces were designed by the restricted approach mentioned earlier to produce the design lift coefficients shown on the figure. Circular-arc profiles of the indicated streamwise thickness ratios were then added symmetrically to the cambered surfaces. For each planform, an uncambered wing with circular-arc sections was tested for comparison.

EXPERIMENTAL RESULTS AND DISCUSSION

The results of the experimental investigation of the drag-due-to-lift characteristics of this family of highly swept arrow wings are shown in figure 6. The experimental values of drag rise factor $\dfrac{C_D}{\beta C_L{}^2}$, represented by the symbols, were obtained from experimental drag polars by use of the expression

$$\left[\frac{C_D}{\beta C_L{}^2}\right]_{experiment} = \frac{C_D \text{ at } C_{L,design} - \left[C_{D,minimum}\right]_{flat\ wing}}{\beta\left(C_{L,design}\right)^2} \tag{5}$$

It can be seen from the figure that the flat-wing results represented by the square symbols lie slightly under the theoretical curve for flat wing neglecting the leading-edge suction force. The drag rise factors for the cambered wings denoted by the circles, although well above the theoretical curves for optimum and restricted camber, do indicate a definite improvement over the flat wings.

The cambered wings with 70° leading-edge sweep and design $C_L = 0.08$ was the only wing which was theoretically subcritical at the design condition, and as indicated on the figure, this wing produced the lowest drag rise factor. It should be pointed out, however, that a design lift coefficient as low as 0.08 is not consistent with optimum flight conditions at $M = 2$ either in the wind-tunnel or full-scale flight at altitude. There are, indeed, smaller differences in the numerator and denominator of equation (5) and therefore considerably greater inaccuracies in the determination of drag rise factor from the experimental

results. It is nevertheless significant that the most probable value of drag rise factor for the subcritical wing is substantially lower than that for the flat wing, but disappointing that there is still a rather large discrepancy indicated between theory and experiment.

From flow pictures taken on the series of restricted cambered wings, there is no longer an indication that the discrepancy between theory and experiment can be attributed to a breakaway in the flow over the upper surface. Figure 7 is representative of the type of flow which occurred on the family of wings under investigation. This oil-film picture taken in the Langley 4-foot supersonic tunnel shows the flow over the upper surface of the 70° restricted cambered wing at $M = 2$ and $C_L \approx 0.16$. For these conditions no leading-edge separation nor tip trailing-edge separation was present. The flow separation visible in the photograph can be attributed to surface irregularities on the wing or air bleeding from the lower surface of the semispan model through the root chord gap.

On the basis of the experimental results and the analysis of flow fields required by linearized theory to produce a low-drag wing, it is concluded that linear theory is not adequate for the design of highly sweptback wings having optimum aerodynamic loading. It appears that the assumptions of the linear theory are strongly violated and that consideration of the nonlinear aerodynamics must be included in a wing design. R. T. Jones in reference 10, commenting on the work of Kogan, reference 15, in which the reversed Mach cone is used as a control sur- face for momentum integrals, indicated that Kogan's general result for optimum loading should be valid to second order. This result gives

encouragement to the hope that low values of drag due to lift are attainable. It is important to note in this connection that Kogan's condition gives values of the potential on the reversed Mach cone control surface which are then valid to second order according to Jones; however, the aerodynamic loading on the wing surface which produces the mentioned potential distribution is undoubtedly considerably affected by inclusion of second-order terms, hence the attainment of the optimum linear loadings may not necessarily produce the desired result. This problem is of considerable interest and warrants additional attention.

CONSIDERATION OF LIFTING FOREBODIES

The foregoing discussion has concentrated primarily on highly swept arrow wings to obtain low values of drag. An alternate approach toward obtaining low drag under lifting conditions is to increase the effective aspect ratio of the wing in both the chordwise and spanwise sense. The so-called area rule as applied to lifting elements leads to this conclusion and some theoretical calculations provide further support to this idea. The basic concept is to design the body or fuselage so that it will carry lift and produce a favorable upwash field over the main wing. Licher (ref. 16) has made a calculation of the drag due to lift of an elliptic planform wing together with an idealized body which illustrates this concept. The body was simply represented by a lift distribution along a line but which carried no net lift. His calculations showed that the drag of this wing-body configuration would be reduced by as much as 30 or 40 percent below the drag of the wing alone, provided the body

- 13 -

could support the required lift. Although it is unlikely that a body can be designed to carry sufficient lift to obtain drag reductions of this magnitude, the concept appears to offer possibilities of sufficient drag reductions to warrant further study. In order to explore this concept further it is necessary to make a more realistic approximation to the lifting body. Since the forebody must carry a substantial amount of lift to effect a sizable drag reduction over that of the wing alone, the body would have to be, in effect, a low-aspect-ratio wing. From the point of view of the lift distribution, then, the wing and lifting body can be regarded as a wing of very general planform.

Of necessity, the calculation of the flow over wings of general planform entails approximate methods even within the framework of linearized theory. Some work oriented in the direction of determining the camber distribution to minimize the drag at a given lift has been presented by Ginzel and Multhopp (ref. 17) and a numerical method for determining the downwash corresponding to a given pressure distribution has been given by Hancock (ref. 18). A method similar in concept but differing in detail from that of Hancock has been developed independently at the Langley Research Center of NASA to optimize the camber and loadings for a given wing planform.

For this purpose the wing planform is divided into a finite number of elements each of which is uniformly loaded and the donwash over a similar element within the region of influence of the first is obtained in analytic form. The equations for the downwash assume the simplest form by employing characteristic coordinates corresponding to a stream Mach number of $\sqrt{2}$. The coordinates are then orthogonal and the finite

elements can be taken as squares whose edges are aligned in the two characteristic coordinate directions. Figure 8 illustrates the mesh arrangement employed in the analysis. The area which includes the wing surface and is bounded by the intersection of the forward and reverse Mach lines is divided into $\bar{n}^2$ elements whose coordinates can be represented by the integers i,j or m,n where $1 \leqq i,j,m,n \leqq \bar{n}$. For those elements which lie along the boundary of the wing planform it is necessary to make a further subdivision of the basic mesh size in order to obtain a satisfactory approximation of the effect of the wing edges on the downwash.

The average value of downwash angle, α, on the area m,n due to unit pressure on the element i,j can be determined from the expression

$$\alpha = \frac{1}{S_{m,n}} \int_{S_{m,n}} (w)_{C_{P_{i,j}}} dS$$

where $S_{m,n}$ is the area of the element m,n and w is the local downwash angle. The total downwash angle at a given element m,n can be obtained by summing the contributions from all the elements of the wing which lie within the upstream Mach lines from the element.

The criterion for minimum drag for a given lift as found by R. T. Jones (ref. 6) is that the combined downwash due to forward and reverse flows is a constant everywhere on the wing. This condition is approximated by requiring that the average value of the combined downwash on each rectilinear element of the wing have a constant value.

- 15 -

Such a procedure leads to a set of simultaneous equations given by

$$\sum_{j=1}^{n} \sum_{i=1}^{m} C_{P_{i,j}} \, \alpha_{i,j}^{m,n} + \sum_{j=n}^{\bar{n}} \sum_{i=m}^{\bar{n}} C_{P_{i,j}} \, \alpha_{m,n}^{i,j} = \text{Constant}$$

which can be solved for the unknown pressure coefficients. With these

values determined, the corresponding shape and drag coefficient can be

evaluated.

Some calculations have been made on this basis wherein up to 100

simultaneous equations were solved on electronic computing equipment to

evaluate the pressure distributions. A comparison with the known analytic

solutions for the minimum-drag sonic-edge triangular wing shows that this

approximate analysis is satisfactory for evaluating the integral spanwise

and chordwise loadings and gives the correct theoretical value of the

minimum value of $\dfrac{C_D}{\beta C_L^2}$. The local pressure and camber distributions

corresponding to the minimum drag value are somewhat less satisfactory,

since these distributions show some irregularity between adjoining span-

wise stations. This irregularity appears to be caused by forcing the

solution toward the condition which produces the minimum theoretical value

of the drag.

A computation of the loading for the planform shown in figure 9 was

made to gain some insight into the possibilities of using the lifting

forebody to create a favorable upwash field over the wing. The forebody

has a uniform loading and the camber of the remaining wing panel was

designed to give minimum drag. The highly swept forebody has subsonic

leading edges and the wing leading edge is sonic. The calculated drag

rise factor for this configuration is approximately 11 percent lower than .

that of a flat-plate wing of the same planform with leading-edge suction (ref. 19). The constant surface loading on the forebody is $1.44c_L$, a value which may be difficult to attain because of nonlinear aerodynamic effects. Nonetheless, it is a hopeful result that even with an inefficient (uniformly loaded) forebody the sonic afterportion of the wing was theoretically able to recover a large amount of energy from the forebody upwash velocity field to effect a net 11-percent decrease in drag. A lifting forebody configuration has, in addition to possible structural advantages, the definite promise of reduced trim drag. These considerations together with the calculated performance improvement indicate the desirability of further experimental and analytical studies of such arrangements.

In conclusion the authors wish to acknowledge the contribution of Mr. H. Carlson of the Langley 4-foot supersonic wind tunnel and the staff of the Langley Unitary Plan wind tunnel in obtaining the experimental results presented.

REFERENCES

1. Brown, C. E., and McLean, F. E.: The Problem of Obtaining High Lift-
   Drag Ratios at Supersonic Speeds. Jour. of Aero. Sci., vol. 26,
   no. 5, pp. 298-302, May 1959.

2. Ferri, A., Vaglio-Lauren, R., and Ness, N.: Mixed Type Conical Flow
   Without Axial Symmetry. PIBAL Report No. 264, Polytechnic Institute
   of Brooklyn, New York, Dec. 1954.

3. Sears, W. R., ed.: High-Speed Aerodynamics and Jet Propulsion, Vol. 6.
   General Theory of High-Speed Aerodynamics. Section E, 8. Princeton
   University Press, 1954, pp. 477-487.

4. Moore, F. K.: Second Approximation to Supersonic Conical Flows. Jour.
   of Aero. Sci. 17, 328, 1950.

5. Tan, H. S.: Second Approximation to Conical Flows. WADC Technical
   Report 52-277, Wright Air Development Center, Dayton, Ohio, USA,
   1952.

6. Jones, Robert T.: The Minimum Drag of Thin Wings in Frictionless Flow.
   Jour. Aero. Sci., vol. 18, no. 2, Feb. 1951, pp. 75-81.

7. Graham, E. W.: The Calculation of Minimum Supersonic Drag by Solution
   of an Equivalent Two-Dimensional Potential Problem. Rep.
   No. SM-22666, Douglas Aircraft Co., December 1956.

8. Zhilin, Yu. L.: Wings of Minimum Drag. Prikladnaia Matematika i
   Mekhanika (Moscow, Leningrad), vol. XXI, pp. 213-220, 1957.

9. Germain, Paul: Sur le Minimum de Trainee d'une Aile de Forme en Plan
   Donnée. Compte Rendus, vol. 244, no. 9, pp. 1135-1138, February 25,
   1957.

10. Jones, Robert T.: Aerodynamic Design for Supersonic Speeds. First International Congress of Aero. Sci., Madrid, Spain. Sept. 8-13, 1958.

11. Katzen, Elliott D.: Idealized Wings and Wing-Bodies at a Mach Number of 3. NACA TN 4361, 1958.

12. Tucker, W. A.: A Method for the Design of Sweptback Wings Warped to Produce Specified Flight Characteristics at Supersonic Speeds. NACA Rep. 1226, 1955.

13. Grant, Frederick C.: The Proper Combination of Lift Loadings for Least Drag on a Supersonic Wing. NACA Rep. 1275, 1956. (Supersedes NACA TN 3533.)

14. Kainer, J. H.: Theoretical Calculations of the Supersonic Pressure Distribution and Wave Drag for a Limited Family of Tapered Sweptback Wings with Symmetrical Parabolic-Arc Sections at Zero Lift. NACA TN 2009, Jan. 1950.

15. Kogan, M. N.: On Bodies of Minimum Drag in a Supersonic Gas Stream. Prikladnaia Matematika y Mechanika, vol. XXI, 1957, pp. 207-212.

16. Licher, R. M.: Reduction of Drag Due to Lift in Supersonic Flight by Distributing Lift Along a Fuselage. Jour. Aero. Sci., vol. 23, no. 11, Nov. 1956, pp. 1037-1043.

17. Ginzel, I., and Multhopp, H.: Wings With Minimum Induced Drag in Supersonic Flow. Martin Company Engineering Report No. 9937-M, August 1957.

18. Hancock, G. J.: Notes on Thin Wing Theory at Low Supersonic Speeds. Aeronautical Research Council A.R.C. 20, 285, July 1958.

19. Cohen, Doris, and Friedman, M. D.: Theoretical Investigation of the Supersonic Lift and Drag of Thin, Sweptback Wings with Increased Sweep Near the Root. NACA TN 2959, June 1953.

FIXED TRANSITION; $C_L \approx 0.1$; $M = 2.87$
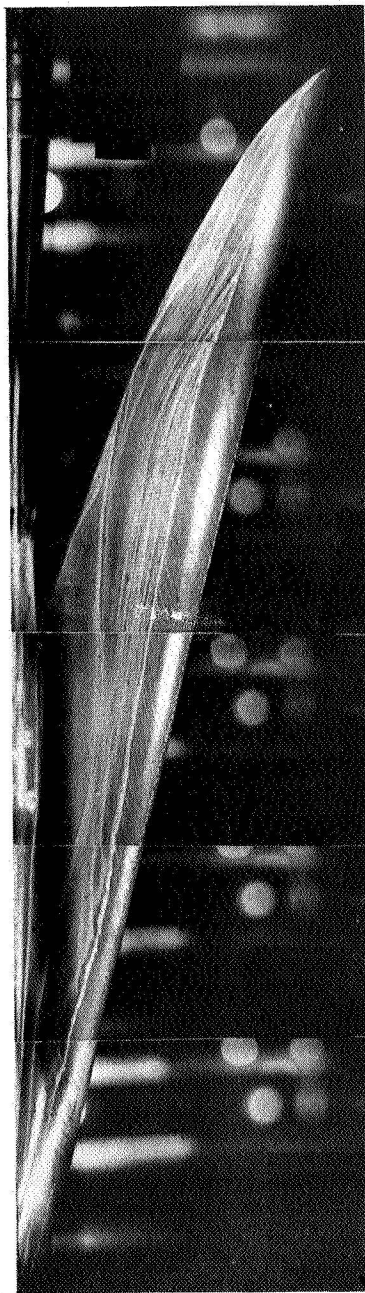
L-58-1676
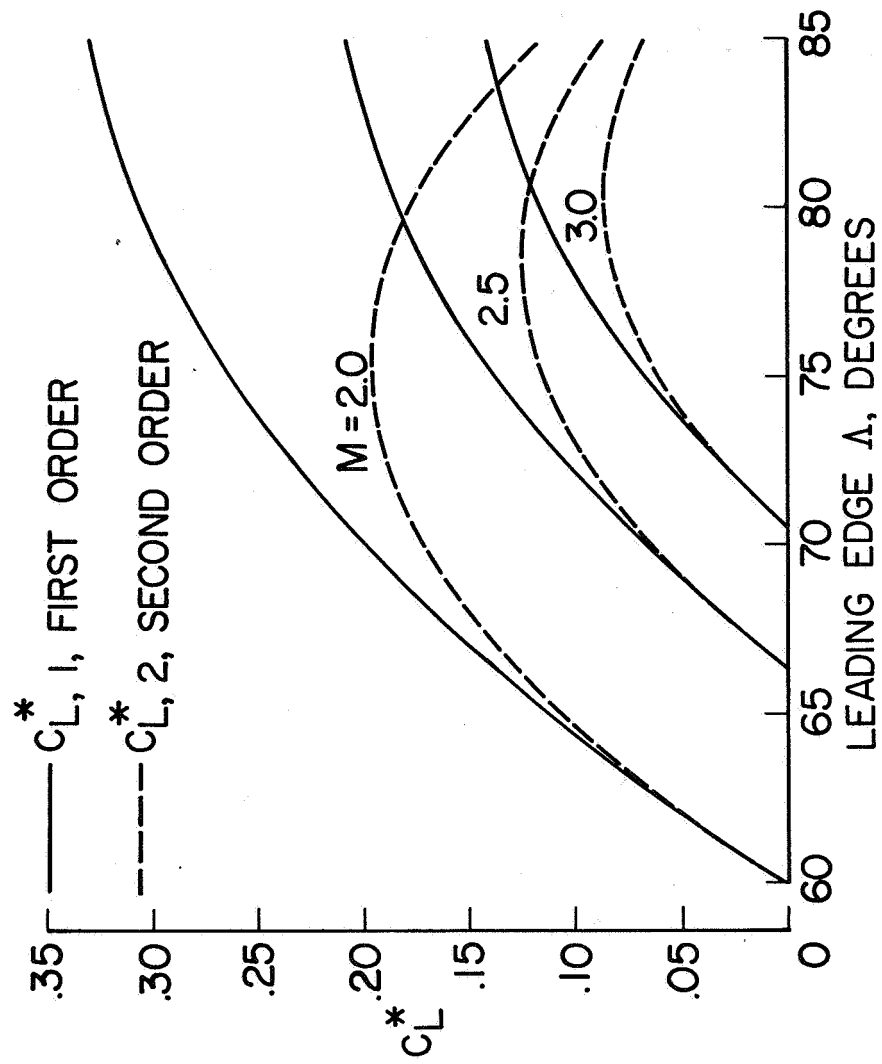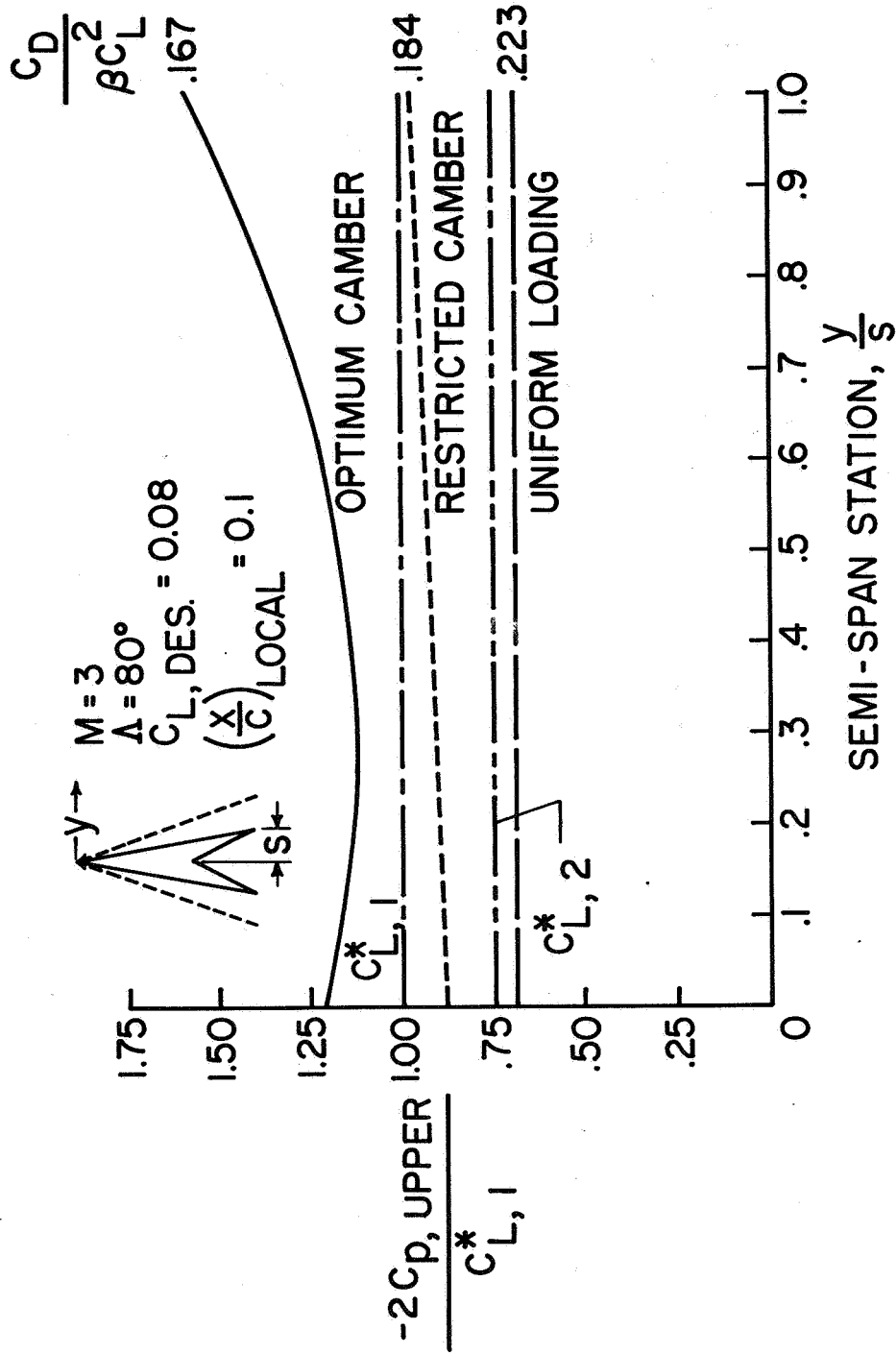NASA

Figure 1.- Oil film flow picture of arrow wing.

Figure 2.- Critical c_L for sweptback wings with uniform loading.

NASA

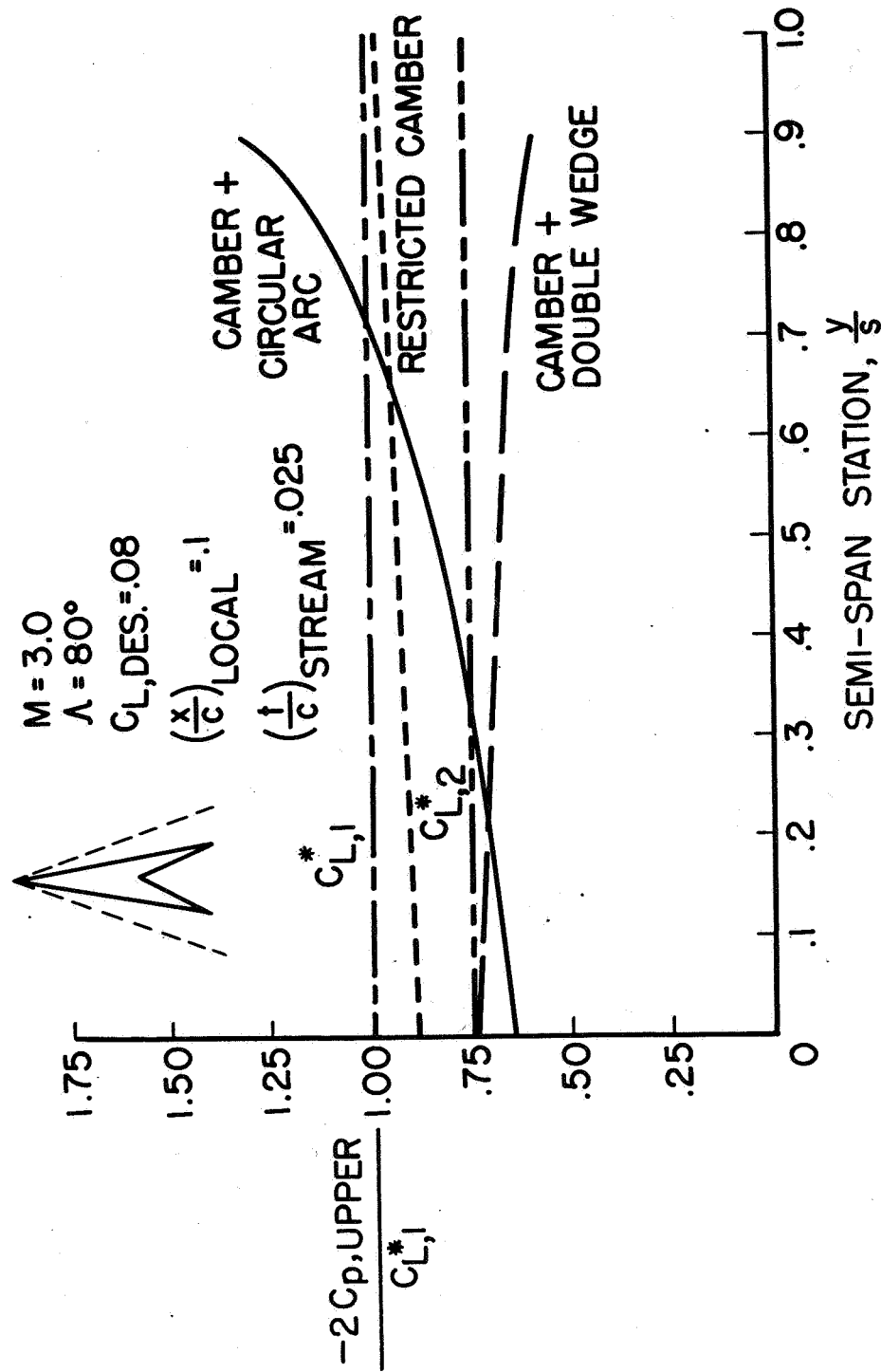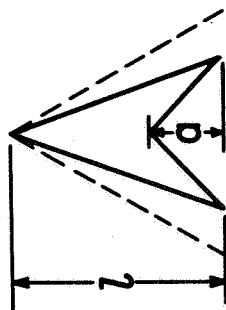Figure 3.- Upper surface pressures near leading edge of cambered wing.

NASA

Figure 4.- Effect of thickness on upper surface pressures.

NASA

$a = .35l$

$M = 2.0 \quad \Lambda = 70°$
$C_{L,DES.} = 0, .08, .16$
CIRCULAR ARC STREAMWISE, $\left(\dfrac{t}{c}\right) = .030$
$\beta \times$ ASPECT RATIO = 3.88

$M = 2.0 \quad \Lambda = 75°$
$C_{L,DES.} = 0, .16$
CIRCULAR ARC STREAMWISE, $\left(\dfrac{t}{c}\right) = .030$
$\beta \times$ ASPECT RATIO = 2.86
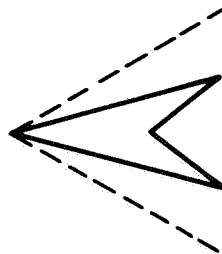
$M = 3.0 \quad \Lambda = 80°$
$C_{L,DES.} = 0, .08$
CIRCULAR ARC STREAMWISE, $\left(\dfrac{t}{c}\right) = .025$
$\beta \times$ ASPECT RATIO = 3.08
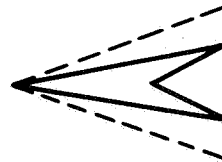
NASA
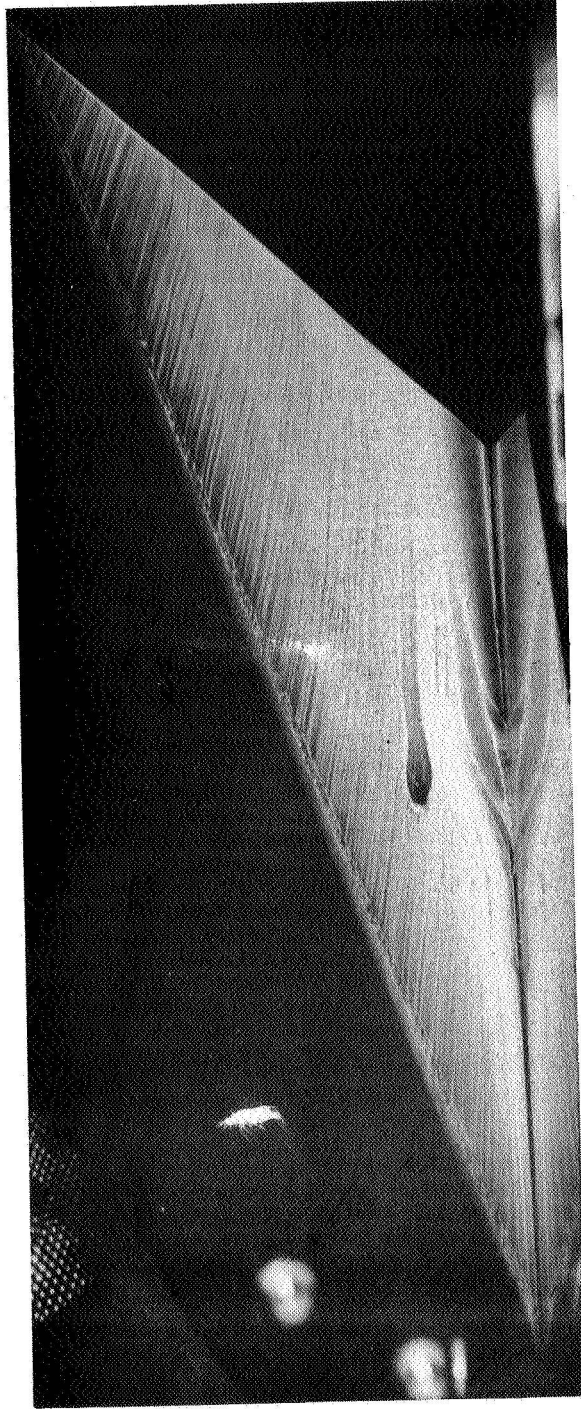
Figure 5.- Planforms and design conditions for experimental tests.
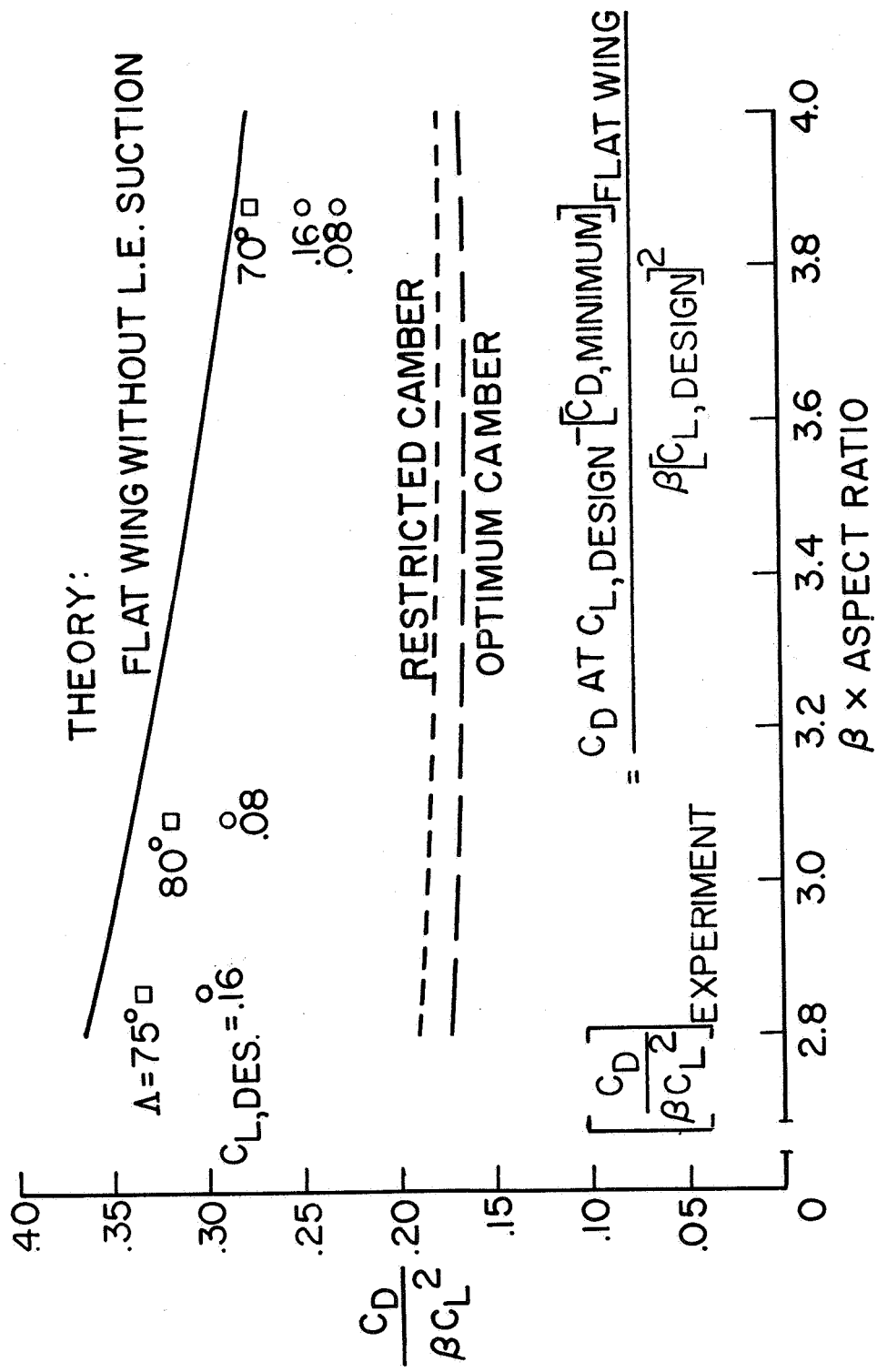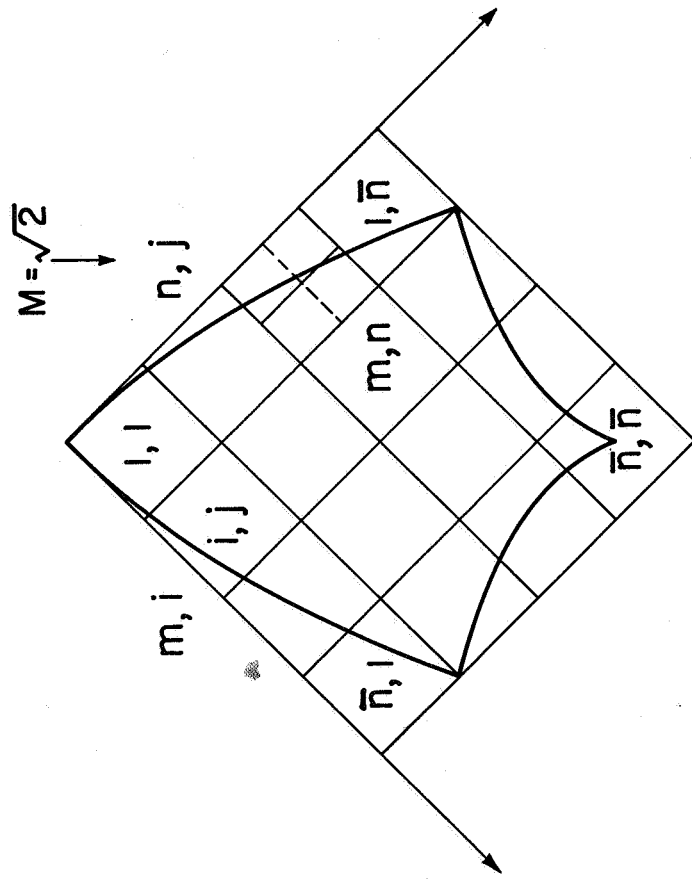
Figure 6.- Theoretical and experimental drag rise factors for arrow wings.

FIXED TRANSITION; $C_L \approx .16$ M = 2.0

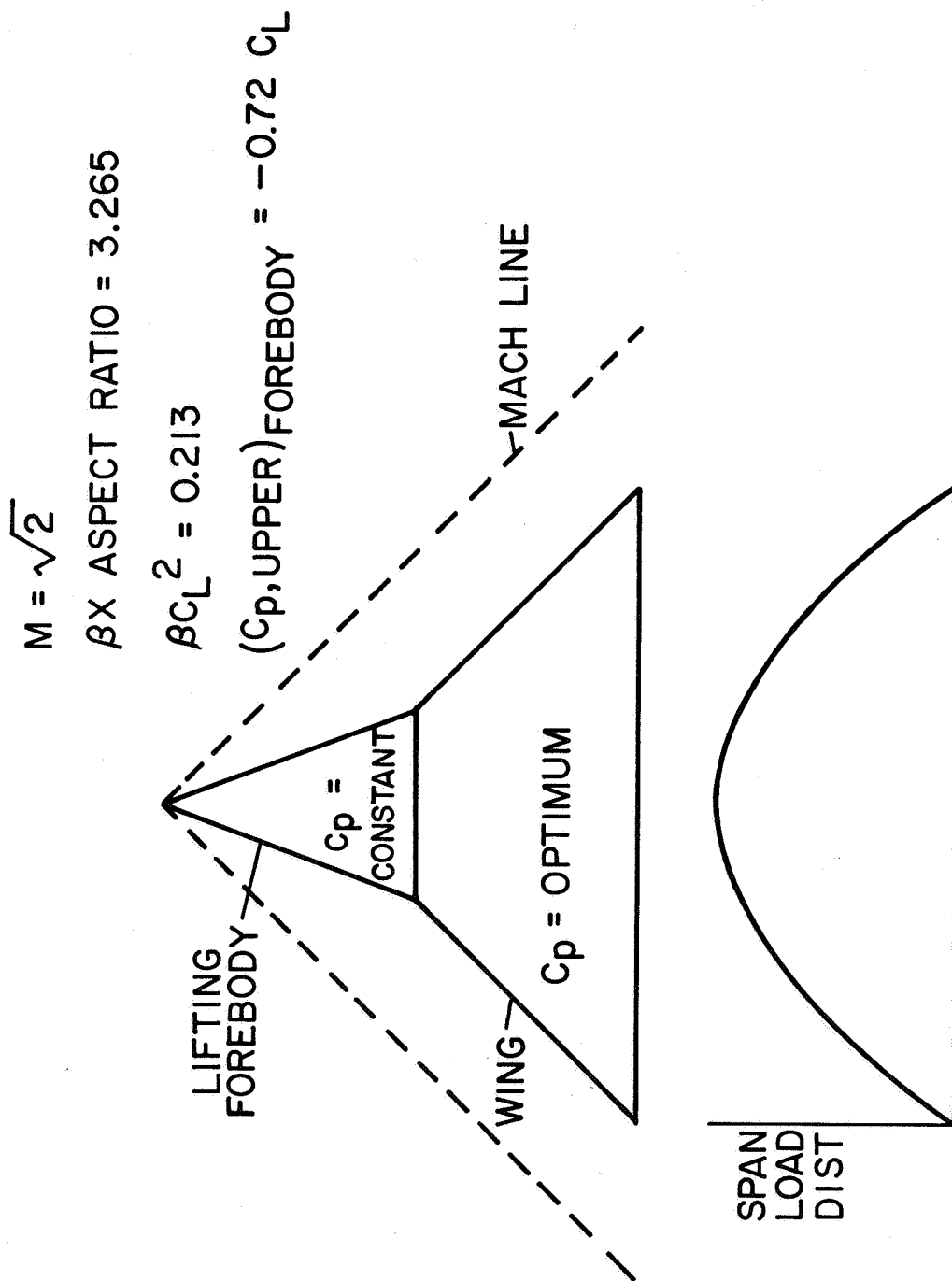Figure 7.- Oil film flow picture of "restricted" arrow wing.

Figure 8.- Mesh arrangement for calculation of arbitrary planform.

NASA

$M = \sqrt{2}$

$\beta \times$ ASPECT RATIO = 3.265

$\beta C_L^2 = 0.213$

$(C_{p,\text{UPPER}})_{\text{FOREBODY}} = -0.72\ C_L$

MACH LINE

LIFTING FOREBODY

C_p = CONSTANT

WING

C_p = OPTIMUM

SPAN LOAD DIST

NASA

Figure 9.- Example of lifting forebody-wing arrangement.